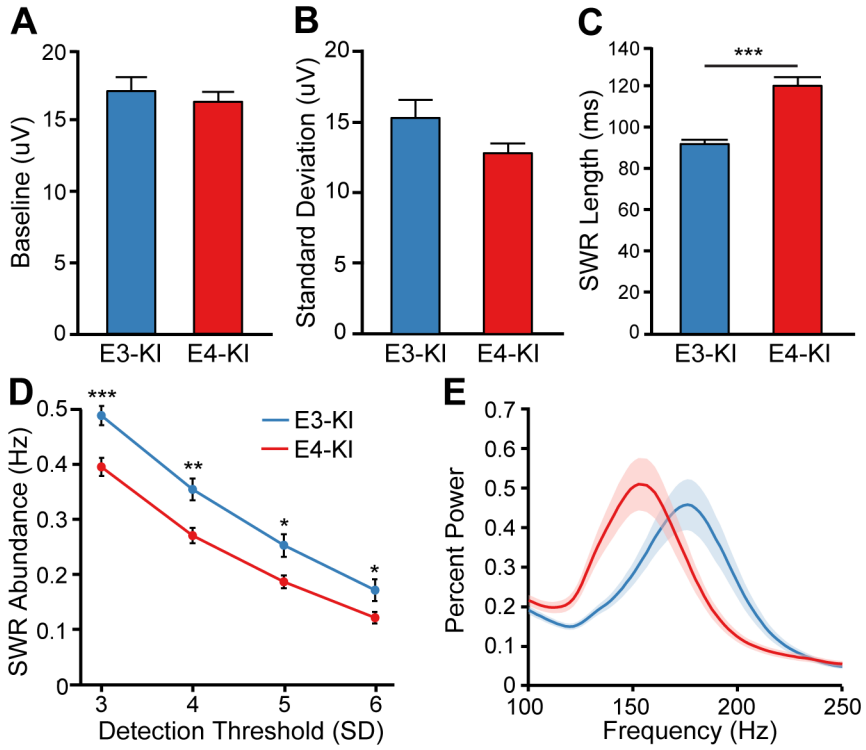

Figure S1. Further characterization of SWR events in aged apoE3-KI and apoE4-KI mice (related to Figure 2).

(A, B) Average baseline value (A) and standard deviation (B) of ripple band-filtered data (150–250 Hz) do not differ between genotype groups.

(C) SWR length (calculated from the time when ripple-filtered data exceeds baseline immediately preceding threshold crossing to the time when it returns to baseline) is greater in aged apoE4-KI mice than in apoE3-KI mice (unpaired *t* test, t(25) = 6.981).

(D) SWR abundance after re-extraction of SWRs with 125–150-Hz ripple frequency band (unpaired *t* tests; t(25) = 3.855, 3.439, 2.724, 2.164 for 3, 4, 5, and 6 SD, respectively)

(E) Percent power spectra of aged apoE3-KI and apoE4-KI mice during ripples, with 125–150-Hz ripple frequency band used for SWR detection. Peak frequency of ripple oscillation was significantly different between genotype groups (unpaired t-test; t(25) = 8.722).

*P<0.05, **P<0.01, ***P < 0.001, n = 14, 13 for apoE3-KI and apoE4-KI, respectively. Error bars and shading indicate SEM.

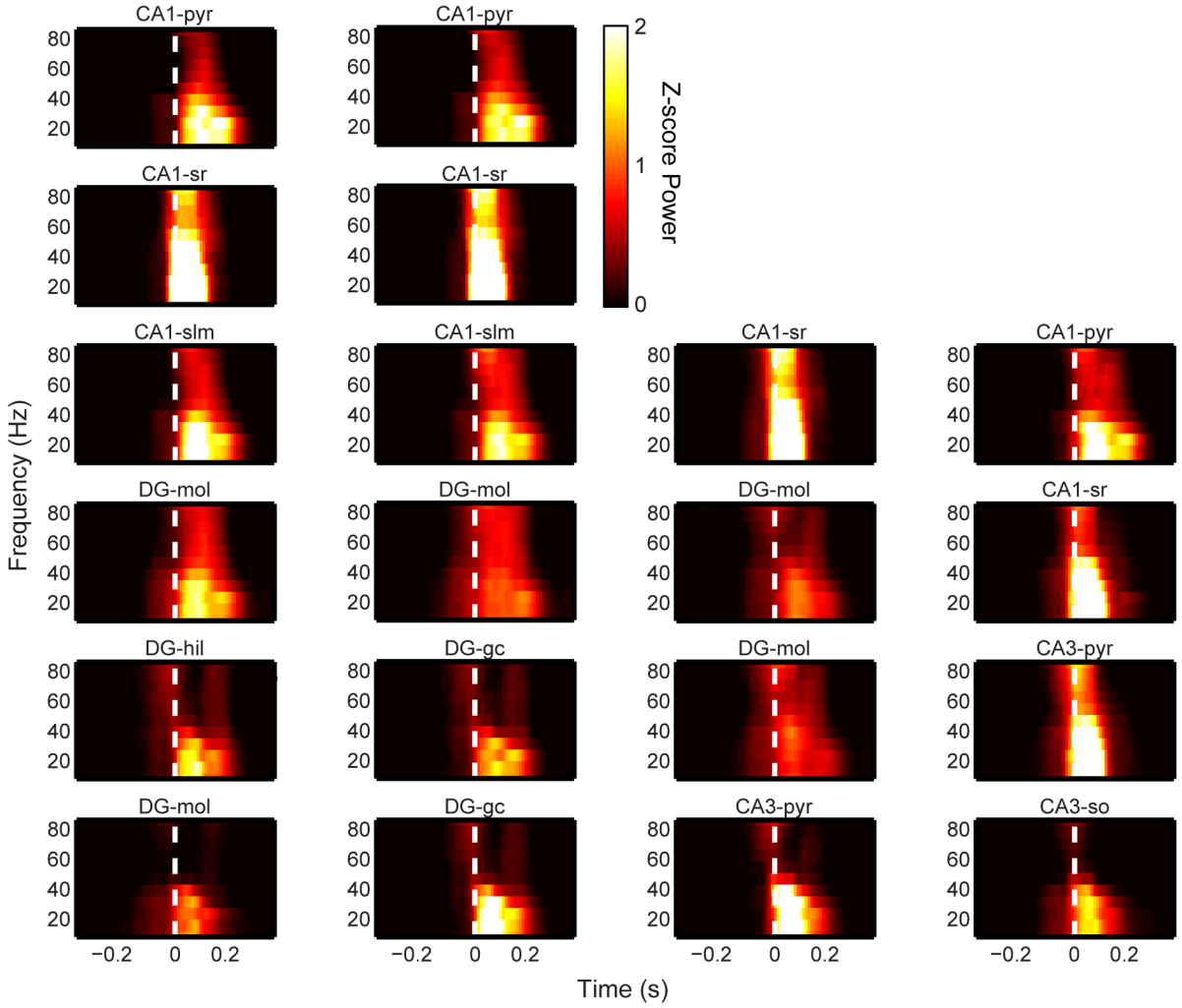

Figure S2. Variability and lack of volume conduction across recording sites, apoE3-KI example (related to Figure 3).

SWR-triggered spectrograms for all hippocampal sites in a representative apoE3-KI mouse show significant variability across neighboring sites and a lack of volume-conducted activity in gamma frequency range. White dashed line represents threshold crossing for SWR detection. Sites include CA1 stratum oriens (CA1-so), CA1 pyramidal cell layer (CA1-pyr), CA1 stratum radiatum (CA1-sr), CA1 stratum lacunosum-moleculare (CA1-slm), CA3 pyramidal cell layer (CA3-pyr), CA3 stratum radiatum (CA3-sr), CA3 stratum oriens (CA3-so), DG molecular layer (DG-mol), DG granule cell layer (DG-gc), and DG hilus (DG-hil).

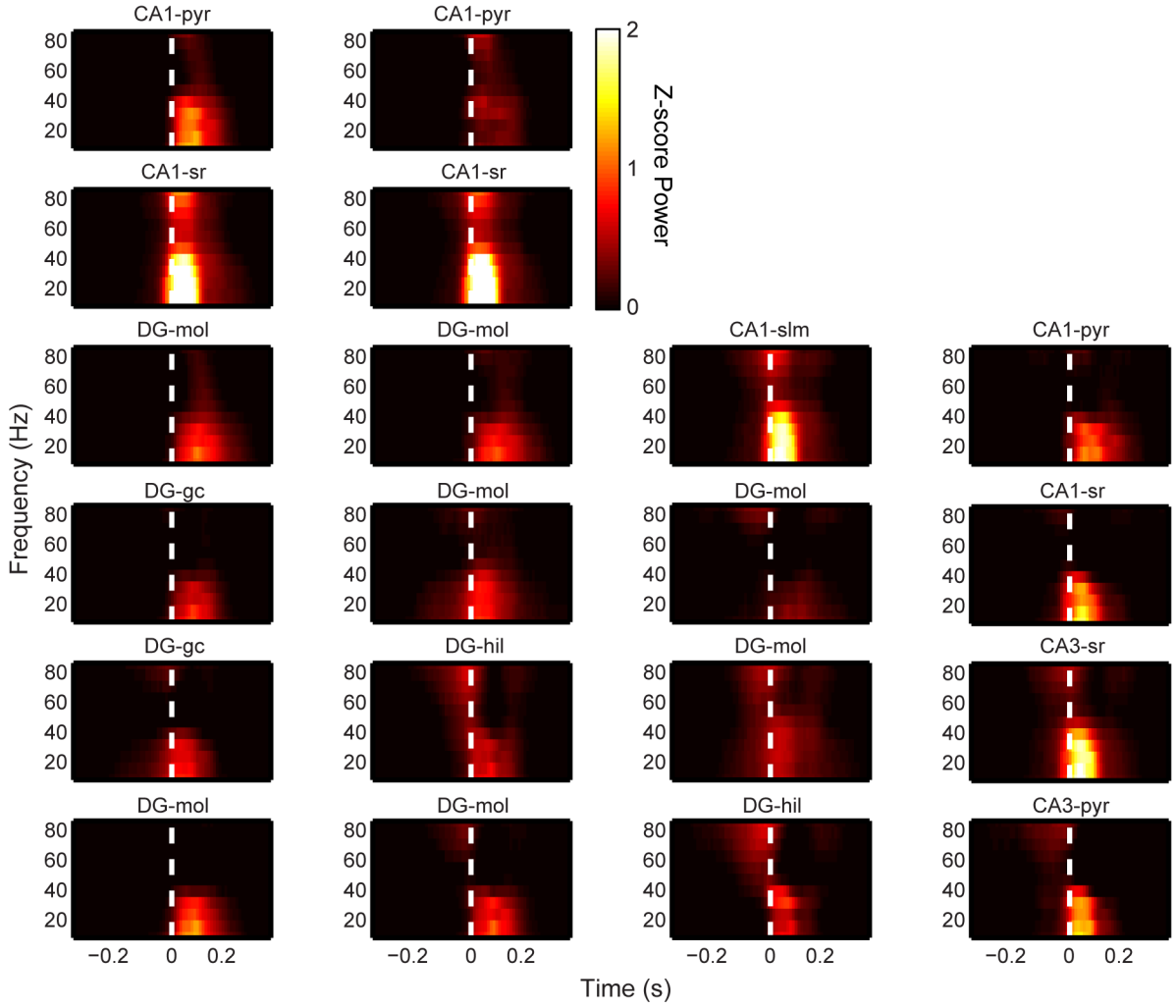

Figure S3. Variability and lack of volume conduction across recording sites, apoE4-KI example (related to Figure 4).

SWR-triggered spectrograms for all hippocampal sites in a representative apoE4-KI mouse show significant variability across neighboring sites and a lack of volume-conducted activity. White dashed line represents threshold crossing for SWR detection. Sites include CA1 stratum oriens (CA1-so), CA1 pyramidal cell layer (CA1-pyr), CA1 stratum radiatum (CA1-sr), CA1 stratum lacunosum-moleculare (CA1-slm), CA3 pyramidal cell layer (CA3-pyr), CA3 stratum radiatum (CA3-sr), CA3 stratum oriens (CA3-so), DG molecular layer (DG-mol), DG granule cell layer (DG-gc), and DG hilus (DG-hil).

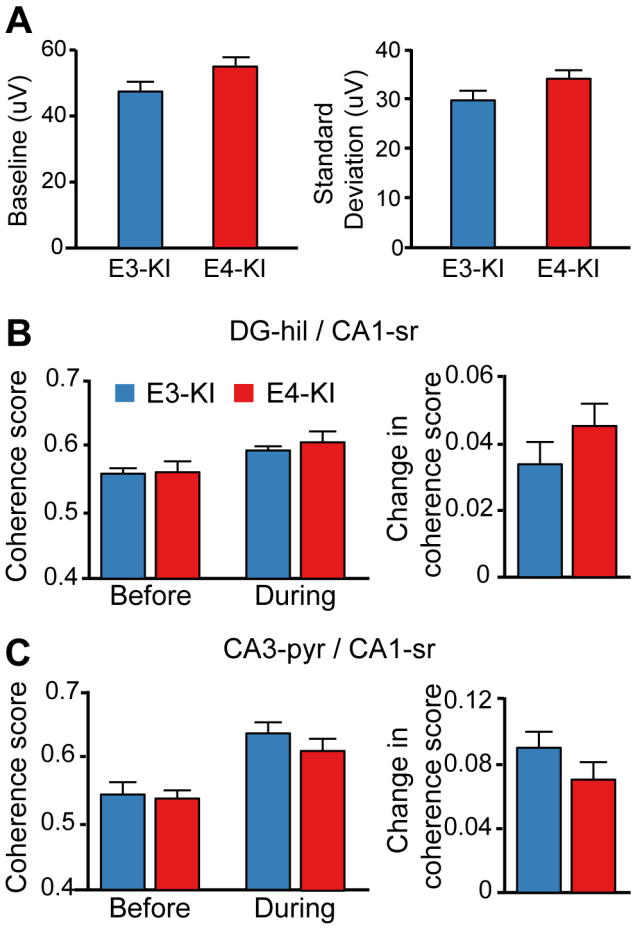

Figure S4. Slow gamma baseline, standard deviation, and coherence in aged apoE3-KI and apoE4-KI mice (related to Figure 4).

(A) Average baseline and standard deviation of slow gamma (30–50 Hz) filtered data during rest periods, excluding SWRs.

(B) Quantification of slow gamma coherence between DG and CA1 stratum radiatum before (400–300 ms before SWR detection) and during (0–100 ms from SWR detection), and the increase between baseline and during SWRs.

(C) Quantification of slow gamma coherence between CA3 and CA1 stratum radiatum before (400–300 ms before SWR detection) and during (0–100 ms from SWR detection), and the increase between baseline and during SWRs.

n = 14, 13 for apoE3-KI and apoE4-KI, respectively. Error bars indicate SEM.

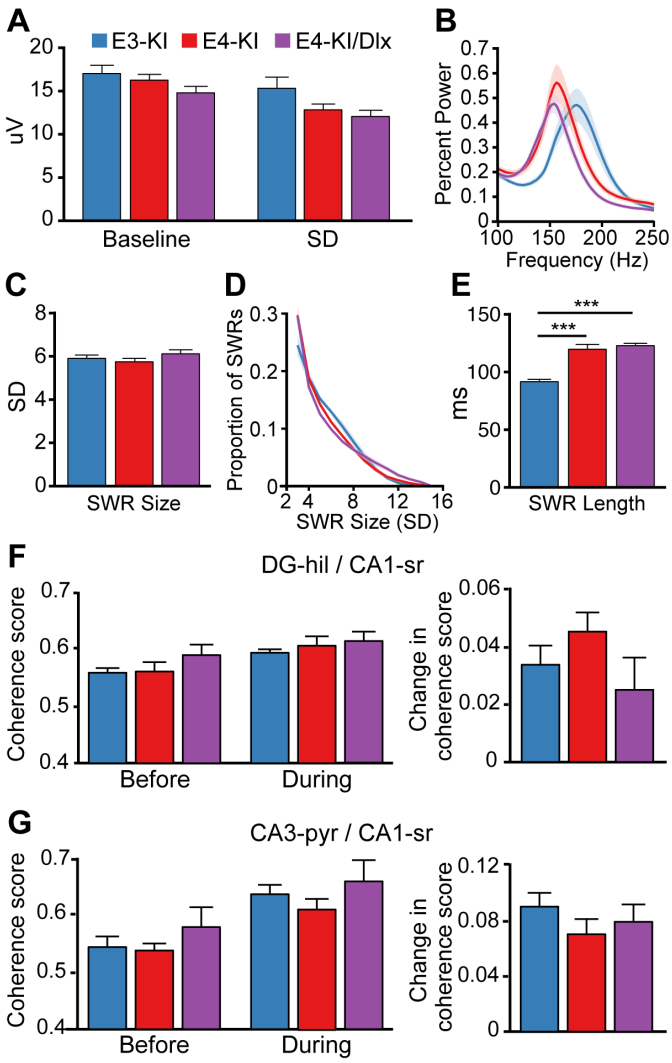

Figure S5. SWR characteristics and slow gamma coherence in aged apoE3-KI, apoE4-KI, and apoE4-KI/Dlx-Cre mice (related to Figure 5).

(A) Average baseline and standard deviation of ripple band-filtered data (150–250 Hz) are not different across aged apoE3-KI, apoE4-KI, and apoE4/Dlx-Cre genotypes.

(B) Percent power spectra of aged apoE3-KI, apoE4-KI, and apoE4-KI/Dlx-Cre mice during SWRs, illustrating peak SWR frequency.

(C) Average SWR size, in units of standard deviation, is not different across the three genotype groups.

(D) Distribution of SWR sizes, in units of standard deviation, is not different across the three genotype groups.

(E) Quantification of average SWR length shows no difference between apoE4-KI and apoE4-KI/Dlx-Cre mice, but both groups have significantly longer events than apoE3-KI mice (one-way ANOVA with corrected post-hoc tests, $F(2,32) = 35.47$.)

(F) Quantification of slow gamma coherence between DG and CA1 stratum radiatum before (400–300ms before SWR detection) and during (0–100ms from SWR detection), and the increase between baseline and during SWRs.

(G) Quantification of slow gamma coherence between CA3 and CA1 stratum radiatum before (400–300ms before SWR detection) and during (0–100ms from SWR detection), and the increase between baseline and during SWRs.

***$P < 0.001$. $n = 14, 13, 8$ for apoE3-KI, apoE4-KI, and apoE4-KI/Dlx-Cre respectively. Error bars indicate SEM.

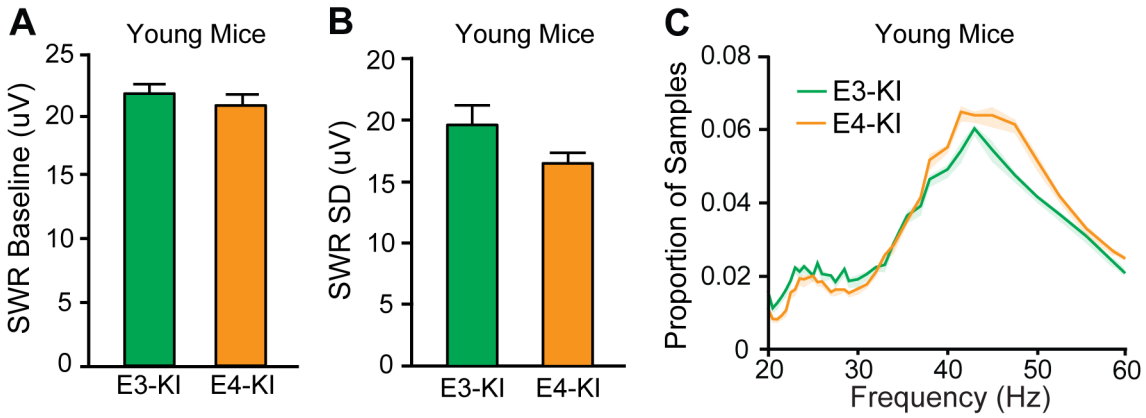

Figure S6. SWR characteristics and slow gamma instantaneous frequency distribution in young apoE3-KI and apoE4-KI mice (related to Figure 6).

(A, B) Average ripple baseline (A) and standard deviation (B) are not different across young genotype groups.

(C) Distribution of instantaneous frequency measurements in CA1 stratum radiatum (CA1-sr) in young apoE3-KI and young apoE4-KI mice.